The arrestin-bound conformation and dynamics of the phosphorylated carboxy-terminal region of rhodopsin

Oleg G. Kisselev[a,*], J. Hugh McDowell[b], Paul A. Hargrave[b,c]

[a] *Departments of Ophthalmology and Biochemistry and Molecular Biology, Saint Louis University School of Medicine, 1755 S. Grand Blvd., St. Louis, MO 63104, USA*
[b] *Department of Ophthalmology, University of Florida, Gainesville, FL, USA*
[c] *Department of Biochemistry and Molecular Biology, University of Florida, Gainesville, FL, USA*

Received 2 December 2003; accepted 23 February 2004

First published online 8 March 2004

Edited by Fritz Winkler and Andreas Engel

Abstract Visual arrestin binds to the phosphorylated carboxy-terminal region of rhodopsin to block interactions with transducin and terminate signaling in the rod photoreceptor cells. A synthetic seven-phospho-peptide from the C-terminal region of rhodopsin, Rh(330–348), has been shown to bind arrestin and mimic inhibition of signal transduction. In this study, we examine conformational changes in this synthetic peptide upon binding to arrestin by high-resolution proton nuclear magnetic resonance (NMR). We show that the peptide is completely disordered in solution, but becomes structured upon binding to arrestin. A control, unphosphorylated peptide that fails to bind to arrestin remains highly disordered. Specific NMR distance constraints are used to model the arrestin-bound conformation. The models suggest that the phosphorylated carboxy-terminal region of rhodopsin, Rh(330–348), undergoes significant conformational changes and becomes structured upon binding to arrestin.

Key words: Rhodopsin; Arrestin; Phosphorylation; Signal termination; Nuclear magnetic resonance

1. Introduction

Deactivation of G protein-coupled receptors occurs through phosphorylation of multiple serine and threonine sites at the carboxy-terminus by specific receptor kinases and subsequent binding of a protein arrestin, which physically prevents interactions between the activated receptor and the G protein [1]. This mechanism has been especially well studied for the interactions between light receptor rhodopsin and visual arrestin [2–4]. Numerous studies have focused on the mechanism of arrestin binding, and conformational changes in the arrestin molecule that are associated with arrestin activation [5,6]. Whether complementary conformational changes occur in the phosphorylated C-terminal region of rhodopsin during rhodopsin–arrestin interactions is unclear. We studied a synthetic polypeptide derived from the C-terminal amino acid sequence of bovine rhodopsin, region Rh(330–348), and chemically phosphorylated at all seven positions, seven-phospho-peptide, 7PP [7], by high-resolution proton nuclear magnetic resonance spectroscopy (NMR). We confirm the extended conformation of this polypeptide in solution and report the arrestin-bound conformation determined by transferred nuclear Overhauser effect (TrNOE) spectroscopy.

2. Materials and methods

2.1. Arrestin and phosphorylated peptide

Arrestin was prepared by the method of Buczylko and Palczewski with modifications as described earlier [8]. Peptide Rh(330–348) from the sequence of bovine rhodopsin was synthesized by standard Fmoc chemistry on an Applied Biosystem model 431A peptide synthesizer. Multiply phosphorylated peptide 7-phospho-Rh(330–348), 7PP, was synthesized on phenylacetamidomethyl polystyrene resin using Boc-O-(diphenylphosphono)-serine and -threonine as described [7]. The peptides were homogeneous by high performance liquid chromatography and showed the expected mass when examined by matrix-assisted laser desorption/ionization time of flight mass spectrometry [7].

2.2. NMR and structure calculations

NMR samples contained 0.16 mM of purified arrestin, 1.77 mM of 7PP, 7-phospho-Rh(330–348) or unphosphorylated Rh(330–348) in sodium phosphate buffer, 0.1 M, pH 6.5 and 10% D_2O in a total volume of 0.6 ml. Two-dimensional high-resolution proton TrNOESY spectra were acquired at 4°C on the Varian Unity-600 spectrophotometer essentially as described earlier [9]. Data were processed off-line using VNMR 5.2. Total correlation spectroscopy [10] (2D TOCSY, MLEV-17 mixing sequence of 120 ms, flanked by two 2 ms trim pulses, 0.5 s preacquisition delay and 1.0 s presaturation), and 2D NOESY [11] (t_{mix} = 250 ms, 2×280×2049 data matrix with 16 scans per t_1, using WATERGATE water suppression protocol) were used for sequence-specific and stereo-specific assignments. Preliminary TrNOESY experiments of 7PP and arrestin utilized a range of t_{mix} from 80 ms to 250 ms. NOE built-up curves were mostly linear up to t_{mix} = 250 ms. In order to minimize indirect magnetization transfer effects, a linear phase of NOE built-up at lower t_{mix} is preferable. However, the intensity of the NOE spectra at lower t_{mix} was very weak. Although some spin diffusion was noticed at t_{mix} = 250 ms, most NOE peak intensities did not saturate and remained roughly proportional to the interproton distances. For example, NH-βH and NH-γH peaks of K339 are stronger than NH-δH by a factor of eight and four respectively. Thus, semi-quantitative analysis is warranted. During standard procedures NOEs are classified into weak, medium and strong based on the peak volume and translated to corresponding interproton distances of 1.9–5.0 Å, 1.9–3.5 Å, and 1.9–2.7 Å respectively. In order to minimize overestimation of interproton distances due to potential artifactual effects of spin diffusion, all medium- and long-range NOEs were classified as weak, with the corresponding distance limit of 1.9–5 Å. Because of the significant contribution of an excess of free peptide to the NOE spectra of 7PP in the presence of arrestin, all strong sequential NOEs were given a distance limit of 1.9–3.5 Å instead of 1.9–2.7 Å, and no dihedral angles ϕ and ψ were restrained based on the sequential NOE intensities, essentially as described before [12]. Earlier results for the C-terminal region of transducin α subunit [9], which utilized similar procedures, were con-

*Corresponding author. Fax: (1)-314-256 3253.
E-mail address: kisselev@slu.edu (O.G. Kisselev).

0014-5793/04/$30.00
doi:10.1016/S0014-5793(04)00226-1

firmed in independent TrNOESY experiments utilizing $t_{mix} = 48$ ms, and structure calculations based on TrNOE and residual dipolar coupling restraints [13]. Structure calculations involved distance geometry (DISTGEOM of TINKER 3.9 [14]), 1000K restrained molecular dynamics and simulated annealing (ANNEAL, 15 ps total time) and structure refinement (NEWTON, 0.001 RMS gradient). Calculations utilized CHARMM forcefield.

3. Results and discussion

The soluble polypeptide Rh(330–348) has been synthesized chemically in fully phosphorylated form (seven-phospho-peptide, 7PP [7]), and shown to duplicate major functions of the native phosphorylated rhodopsin. 7PP inhibited phototransduction from photoactivated unphosphorylated rhodopsin in the presence of arrestin [15], and induced conformational changes in arrestin typically observed upon interaction of arrestin with native phosphorylated rhodopsin [8]. These results show that major structural features of the phosphorylated C-terminal region of rhodopsin are preserved in 7PP, and that it can be used to study structural dynamics of the rhodopsin–arrestin interface and the mechanism of the signal shut-off.

Sections of ^{1}H-TOCSY and ^{1}H-NOESY spectra of 7PP with or without bovine arrestin are overlaid in Fig. 1. The continuous line in the NH-αH region (4.0–4.6 ppm) shows sequential connectivity interrupted only at P347. Sequence-specific and stereospecific assignment of NOE peaks was done using standard procedures [9,12,16]. Proton resonance assignments in ppm are given in Table 1.

Consistent with previous NMR studies [17,18], 7PP in solution is highly disordered. The NOESY spectrum of 7PP without arrestin shows no indications of structuring of this peptide in solution. Many sequential NOEs in the NH-aliphatic region are very weak, suggesting high flexibility of the side chains. No meaningful medium- or long-range NOEs were identified for free 7PP in solution. This result is also consistent with available X-ray structures of rhodopsin [19], in which unphosphorylated Rh(330–348) is largely extended with a 328–333 region unresolved, and a site-directed spin labeling study [20], which shows that the rhodopsin C-terminal region is highly disordered and mobile.

After addition of arrestin, proton chemical shifts remained essentially unchanged. Line width broadening in the presence of arrestin was considerable, consistent with fast exchange between free and bound forms. The exchange rate between free and arrestin-bound forms of 7PP appears faster or similar to the cross-relaxation rate in the bound state. N-terminal amides of D330 and D331 are not observed due to the fast exchange with solvent. βH protons of the phosphorylated threonines overlap with the corresponding αH protons. Meth-

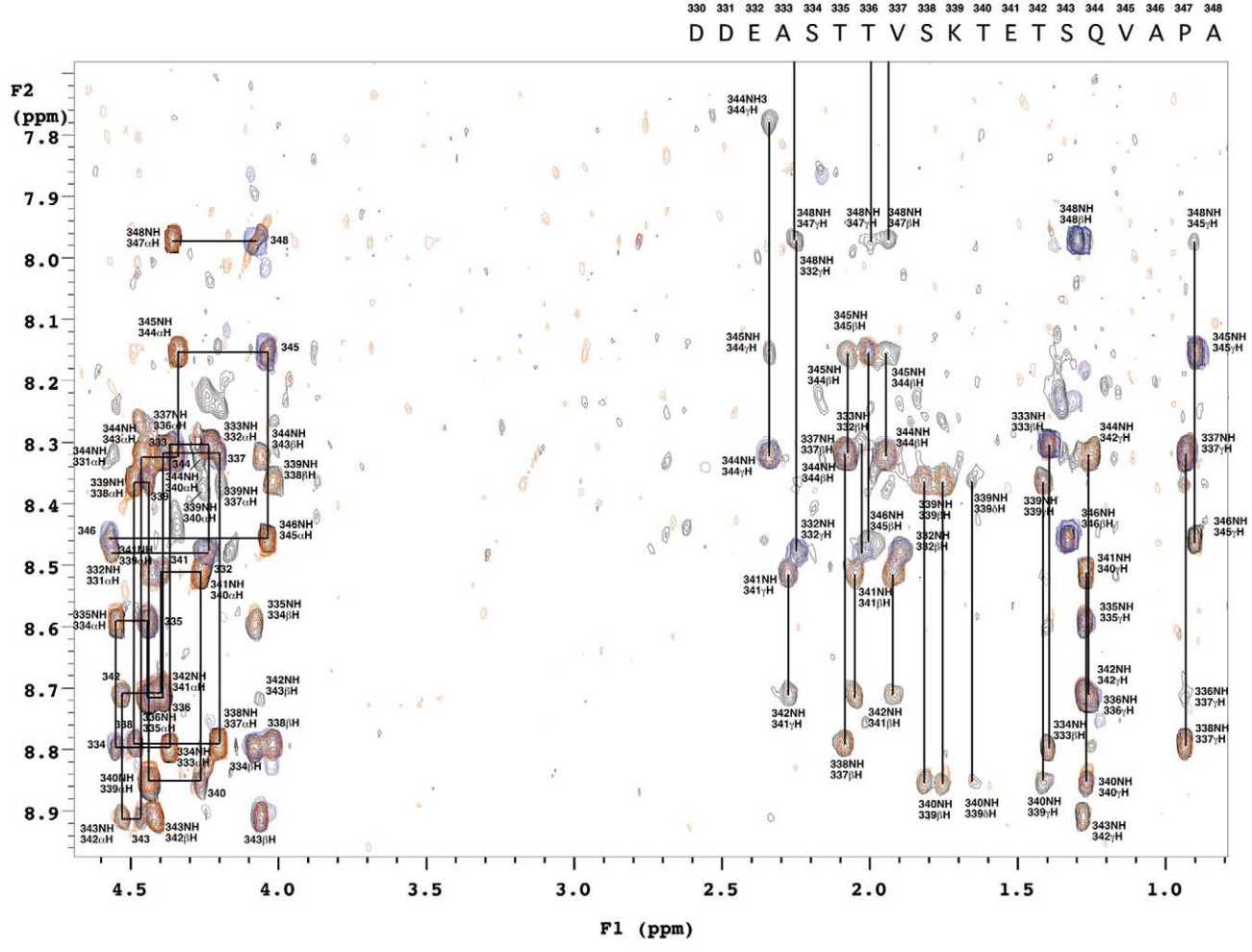

Fig. 1. Sections of ^{1}H-TOCSY (blue) and ^{1}H-NOESY spectra of 7PP in the absence (red) and in the presence (black) of bovine arrestin. The amino acid sequence of 7PP is shown. Serine and threonine residues are phosphorylated.

Table 1
Proton resonance assignments, in ppm

Atom	9	H	Asp	330	N/A
Atom	10	HA	Asp	330	N/A
Atom	11	1HB	Asp	330	2.825
Atom	12	2HB	Asp	330	2.730
Atom	22	H	Asp	331	N/A
Atom	23	HA	Asp	331	4.562
Atom	24	1HB	Asp	331	2.622
Atom	25	2HB	Asp	331	2.563
Atom	36	H	Glu	332	8.480
Atom	37	HA	Glu	332	4.240
Atom	38	1HB	Glu	332	2.023
Atom	39	2HB	Glu	332	1.898
Atom	40	1HG	Glu	332	2.250
Atom	41	2HG	Glu	332	2.250
Atom	48	H	Ala	333	8.300
Atom	49	HA	Ala	333	4.370
Atom	50	1HB	Ala	333	1.396
Atom	51	2HB	Ala	333	1.396
Atom	52	3HB	Ala	333	1.396
Atom	59	H	Ser	334	8.797
Atom	60	HA	Ser	334	4.550
Atom	61	1HB	Ser	334	4.080
Atom	62	2HB	Ser	334	4.080
Atom	71	H	Thr	335	8.591
Atom	72	HA	Thr	335	4.445
Atom	73	HB	Thr	335	4.430
Atom	74	1HG	Thr	335	1.271
Atom	75	1HG2	Thr	335	1.271
Atom	85	H	Thr	336	8.716
Atom	86	HA	Thr	336	4.395
Atom	87	HB	Thr	336	4.380
Atom	88	1HG	Thr	336	1.263
Atom	89	1HG2	Thr	336	1.263
Atom	99	H	Val	337	8.318
Atom	100	HA	Val	337	4.199
Atom	101	HB	Val	337	2.085
Atom	102	1HG1	Val	337	0.931
Atom	103	2HG1	Val	337	0.931
Atom	104	3HG1	Val	337	0.931
Atom	105	1HG2	Val	337	0.931
Atom	106	2HG2	Val	337	0.931
Atom	107	3HG2	Val	337	0.931
Atom	114	H	Ser	338	8.791
Atom	115	HA	Ser	338	4.490
Atom	116	1HB	Ser	338	4.020
Atom	117	2HB	Ser	338	4.020
Atom	128	H	Lys	339	8.364
Atom	129	HA	Lys	339	4.440
Atom	130	1HB	Lys	339	1.819
Atom	131	2HB	Lys	339	1.753
Atom	132	1HG	Lys	339	1.415
Atom	133	2HG	Lys	339	1.415
Atom	134	1HD	Lys	339	1.652
Atom	135	2HD	Lys	339	1.652
Atom	136	1HE	Lys	339	2.930
Atom	137	2HE	Lys	339	2.930
Atom	138	1HZ	Lys	339	7.080
Atom	139	2HZ	Lys	339	7.080
Atom	140	3HZ	Lys	339	7.080
Atom	148	H	Thr	340	8.851
Atom	149	HA	Thr	340	4.261
Atom	150	HB	Thr	340	4.260
Atom	151	1HG	Thr	340	1.270
Atom	152	1HG2	Thr	340	1.270
Atom	164	H	Glu	341	8.512
Atom	165	HA	Glu	341	4.398
Atom	166	1HB	Glu	341	2.050
Atom	167	2HB	Glu	341	1.922
Atom	168	1HG	Glu	341	2.271
Atom	169	2HG	Glu	341	2.271
Atom	178	H	Thr	342	8.708
Atom	179	HA	Thr	342	4.530
Atom	180	HB	Thr	342	4.529
Atom	181	1HG	Thr	342	1.261
Atom	182	1HG2	Thr	342	1.261
Atom	191	H	Ser	343	8.910
Atom	192	HA	Ser	343	4.463
Atom	193	1HB	Ser	343	4.060
Atom	194	2HB	Ser	343	4.060
Atom	205	H	Gln	344	8.323
Atom	206	HA	Gln	344	4.338
Atom	207	1HB	Gln	344	2.082
Atom	208	2HB	Gln	344	1.946
Atom	209	1HG	Gln	344	2.341
Atom	210	2HG	Gln	344	2.341
Atom	211	1HE2	Gln	344	7.780
Atom	212	2HE2	Gln	344	6.830
Atom	220	H	Val	345	8.154
Atom	221	HA	Val	345	4.037
Atom	222	HB	Val	345	2.006
Atom	223	1HG1	Val	345	0.900
Atom	224	2HG1	Val	345	0.900
Atom	225	3HG1	Val	345	0.900
Atom	226	1HG2	Val	345	0.900
Atom	227	2HG2	Val	345	0.900
Atom	228	3HG2	Val	345	0.900
Atom	234	H	Ala	346	8.453
Atom	235	HA	Ala	346	4.570
Atom	236	1HB	Ala	346	1.332
Atom	237	2HB	Ala	346	1.332
Atom	238	3HB	Ala	346	1.332
Atom	246	HA	Pro	347	4.360
Atom	247	1HB	Pro	347	1.936
Atom	248	2HB	Pro	347	2.257
Atom	249	1HG	Pro	347	1.997
Atom	250	2HG	Pro	347	1.997
Atom	251	1HD	Pro	347	3.700
Atom	252	2HD	Pro	347	3.568
Atom	258	H	Ala	348	7.972
Atom	259	HA	Ala	348	4.074
Atom	260	1HB	Ala	348	1.296
Atom	261	2HB	Ala	348	1.296
Atom	262	3HB	Ala	348	1.296

ylene protons exhibited significant chemical shift degeneracy likely because of the equilibration between their nuclear spin magnetizations, and despite acquisition of the NOESY spectra at a ^{1}H frequency of 600 MHz.

In contrast to the free form, in the presence of arrestin, sequential NH-aliphatic interactions in 7PP are strong, especially in the C-terminal portion of the peptide, residues 339–348. A total of 198 constraints were identified and used for structure calculations of the arrestin-bound conformation (Fig. 2a). In order to identify biologically relevant conformations of 7PP in the arrestin-bound state, the structure calculations based on the NMR-derived constraints were performed on the full set of X-ray coordinates of rhodopsin [19] with unresolved parts of loop C3 and the C-terminal region rebuilt in Insight II. The starting conformation of a rebuilt C-terminal region was mostly extended. Only region Rh(324–348) was allowed to move during calculations. This procedure has the benefit of visualizing arrestin-induced conformational changes in the context of the whole receptor and provides a more focused conformational search. Fifteen low-energy models out of 100 independently calculated NMR structures were superimposed using main chain atoms. Coordinates of the average structure and an ensemble of 15 structures of the Rh(330–348) region corresponding to 7PP were deposited in PDB, under number 1NZS.

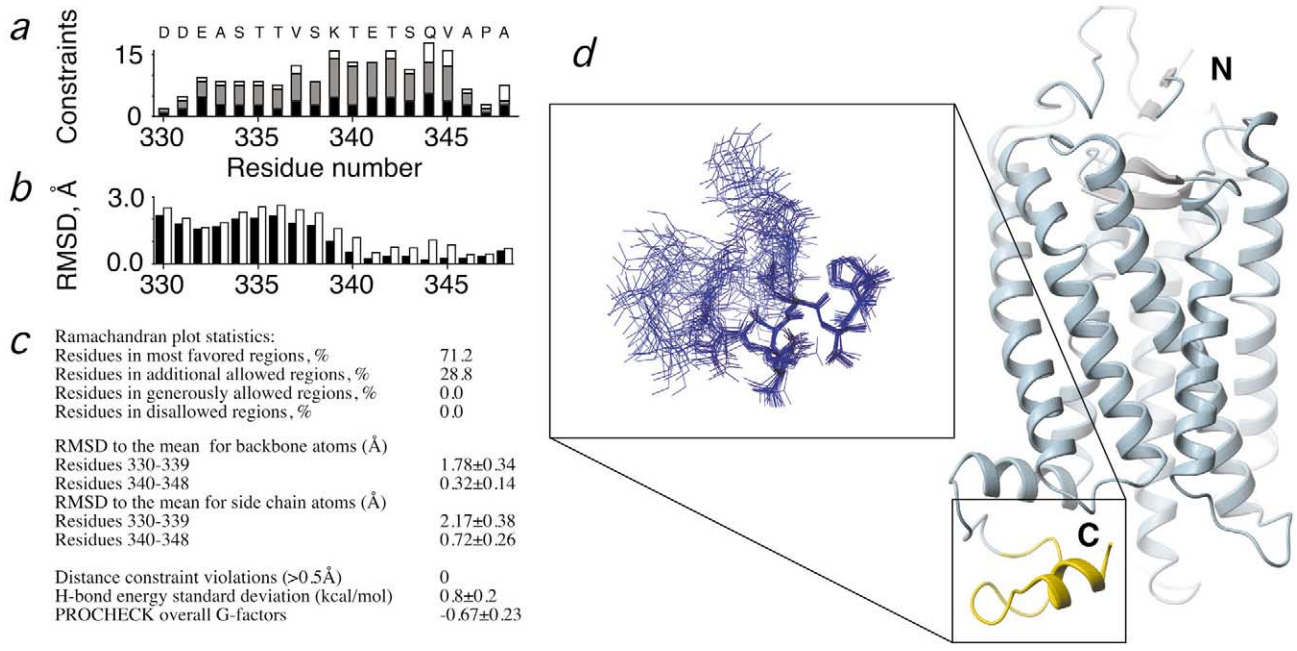

Fig. 2. NMR structures of the phosphorylated C-terminal domain of the bovine rhodopsin in the arrestin-bound state. a: Summary of the experimental distance constraints. Black bar, intraresidue; gray, sequential; white, long-range NOEs. b: Root mean square deviation, RMSD, between individual NMR structures in the final ensemble. Black bar, main chain atoms; white bar, side chain atoms. c: Structural statistics determined by PROCHECK-NMR. d: Lowest energy NMR structure of 7PP, 7-phospho-Rh(330–348), in yellow as part of an X-ray structure of rhodopsin [19] shown as a ribbon model. The N- and C-termini of rhodopsin are labeled. Inset: Final ensemble of the 15 NMR structures superimposed using main chain atoms. There was no NMR evidence of arrestin-induced conformational changes for a control unphosphorylated version of 7PP studied under the same experimental conditions.

Calculations based on the NMR-derived restraints show that the N-terminus of the polypeptide remains flexible. However, the C-terminal region forms a stable helix-loop structure in a manner that brings the N- and the C-termini of 7PP close to each other (Fig. 2d). The overall hairpin fold of arrestin-bound 7PP is supported by the long-range NOEs 348NH-332γH, 344NH-331αH, and 347αH-333βH. Because of the potential overlap of 348NH-332γH with 348NH-347γH, and of 344NH-331αH with 346NH-331αH, these peaks cannot be assigned unambiguously, and the corresponding distance restraints were excluded from the final distance matrix. The C-terminal helix is consistent with a full set of sequential NH–NH interactions, *i*,*i*+2 NOEs 343NH-341NH and 345NH-343NH, NOE peak of an NH-αH (*i*,*i*+4) type, 344NH-340αH, and strong 348–345 *i*,*i*+3 side chain interactions. In addition, two H-bonds of an *i*,*i*+4 type were identified between main chain O and NH of 341–345 and 344–348 respectively during structure calculations, and corresponding additional restraints of 1.9–2.1 Å were introduced during final structure refinement. In the final ensemble of 15 NMR structures produced by independent calculations in the context of the whole rhodopsin, the root mean square deviation, RMSD, an indicator of how close the calculated structures are to each other, shows poor convergence at the N-terminal region 330–339 with RMSD for the main chain atoms of 1.78 ± 0.34 Å and 2.17 ± 0.38 Å for the side chains. In contrast, the C-terminal helical region 340–348 is highly compact with RMSDs 0.32 ± 0.14 Å and 0.67 ± 0.23 Å for the main and side chain atoms respectively (Fig. 2b).

The results show that the seven-phospho-Rh(330–348) peptide, 7PP, undergoes significant conformational changes upon binding to arrestin. Because 7PP mimics major functions of the native phosphorylated rhodopsin, such as induction of the active conformation of arrestin, and inhibition of phototransduction, conformational changes identified in this study are likely to occur during rhodopsin–arrestin binding.

4. Coordinates

Atomic coordinates for the arrestin-bound C-terminal region of rhodopsin have been deposited in the Protein Data Bank (accession code 1NZS).

Acknowledgements: We thank Dr. Anatol Arendt for preparation of rhodopsin C-terminal peptides, both unphosphorylated and phosphorylated, J. Kao for help in recording the NMR spectra and Dr. Art Edison for the critical reading of the manuscript. This work was supported in part by the Norman J. Stupp Foundation, NIH GM63203 and the Foundation for Research to Prevent Blindness (to O.G.K.), and NIH EY06225 and an award from Research to Prevent Blindness (to P.A.H.).

References

[1] Luttrell, L.M. and Lefkowitz, R.J. (2002) J. Cell Sci. 115, 455–465.
[2] Kennedy, M.J., Lee, K.A., Niemi, G.A., Craven, K.B., Garwin, G.G., Saari, J.C. and Hurley, J.B. (2001) Neuron 31, 87–101.
[3] Arshavsky, V.Y. (2002) Trends Neurosci. 25, 124–126.
[4] Maeda, T., Imanishi, Y. and Palczewski, K. (2003) Prog. Retin. Eye Res. 22, 417–434.
[5] Han, M., Gurevich, V.V., Vishnivetskiy, S.A., Sigler, P.B. and Schubert, C. (2001) Structure 9, 869–880.
[6] Vishnivetskiy, S.A., Hirsch, J.A., Velez, M.G., Gurevich, Y.V. and Gurevich, V.V. (2002) J. Biol. Chem. 277, 43961–43967.
[7] Arendt, A., McDowell, J.H., Abdulaeva, G. and Hargrave, P.A. (1996) Protein Peptide Lett. 3, 361–368.
[8] Puig, J., Arendt, A., Tomson, F.L., Abdulaeva, G., Miller, R.,

Hargrave, P.A. and McDowell, J.H. (1995) FEBS Lett. 362, 185–188.
[9] Kisselev, O.G., Kao, J., Ponder, J.W., Fann, Y.C., Gautam, N. and Marshall, G.R. (1998) Proc. Natl. Acad. Sci. USA 95, 4270–4275.
[10] Braunschweiler, L. and Ernst, R.R. (1983) J. Magn. Reson. 53, 521–528.
[11] Kumar, A., Ernst, R.R. and Wüthrich, K. (1980) Biochem. Biophys. Res. Commun. 95, 1–6.
[12] Kisselev, O.G. and Downs, M.A. (2003) Structure 11, 367–373.
[13] Koenig, B.W., Kontaxis, G., Mitchell, D.C., Louis, J.M., Litman, B.J. and Bax, A. (2002) J. Mol. Biol. 322, 441–461.
[14] Hodsdon, M.E., Ponder, J.W. and Cistola, D.P. (1996) J. Mol. Biol. 264, 585–602.
[15] McDowell, J.H., Smith, W.C., Miller, R.L., Popp, M.P., Arendt, A., Abdulaeva, G. and Hargrave, P.A. (1999) Biochemistry 38, 6119–6125.
[16] Wüthrich, K. (1986) NMR of Proteins and Nucleic Acids, Wiley, New York.
[17] Dorey, M., Hargrave, P.A., McDowell, J.H., Arendt, A., Vogt, T., Bhawsar, N., Albert, A.D. and Yeagle, P.L. (1999) Biochim. Biophys. Acta 1416, 217–224.
[18] Getmanova, E. et al. (2004) Biochemistry 43, 1126–1133.
[19] Palczewski, K. et al. (2000) Science 289, 739–745.
[20] Langen, R., Cai, K., Altenbach, C., Khorana, H.G. and Hubbell, W.L. (1999) Biochemistry 38, 7918–7924.